Collisional relaxation of apocarotenals: identifying the S* state with vibrationally excited molecules in the ground electronic state S_0*†

Florian Ehlers,[a] Mirko Scholz,[b] Jens Schimpfhauser,[c] Jürgen Bienert,[c] Kawon Oum*[b] and Thomas Lenzer*[b]

In recent work, we demonstrated that the S* signal of β-carotene observed in transient pump–supercontinuum probe absorption experiments agrees well with the independently measured steady-state difference absorption spectrum of vibrationally hot ground state molecules S_0* in solution, recorded at elevated temperatures (Oum *et al.*, *Phys. Chem. Chem. Phys.*, 2010, **12**, 8832). Here, we extend our support for this ''vibrationally hot ground state model'' of S* by experiments for the three terminally aldehyde-substituted carotenes β-apo-12′-carotenal, β-apo-4′-carotenal and 3′,4′-didehydro-β,ψ-caroten-16′-al (''torularhodinaldehyde'') which were investigated by ultrafast pump–supercontinuum probe spectroscopy in the range 350–770 nm. The apocarotenals feature an increasing conjugation length, resulting in a systematically shorter S_1 lifetime of 192, 4.9 and 1.2 ps, respectively, in the solvent *n*-hexane. Consequently, for torularhodinaldehyde a large population of highly vibrationally excited molecules in the ground electronic state is quickly generated by internal conversion (IC) from S_1 already within the first picosecond of relaxation. As a result, a clear S* signal is visible which exhibits the same spectral characteristics as in the aforementioned study of β-carotene: a pronounced $S_0 \rightarrow S_2$ red-edge absorption and a ''finger-type'' structure in the $S_0 \rightarrow S_2$ bleach region. The cooling process is described in a simplified way by assuming an initially formed vibrationally very hot species S_0** which subsequently decays with a time constant of 3.4 ps to form a still hot S_0* species which relaxes with a time constant of 10.5 ps to form S_0 molecules at 298 K. β-Apo-4′-carotenal behaves in a quite similar way. Here, a single vibrationally hot S_0* species is sufficient in the kinetic modeling procedure. S_0* relaxes with a time constant of 12.1 ps to form cold S_0. Finally, no S_0* features are visible for β-apo-12′-carotenal. In that case, the $S_1 \rightarrow S_0$ IC process is expected to be roughly 20 times slower than S_0* relaxation. As a result, no spectral features of S_0* can be found, because there is no chance that a detectable concentration of vibrationally hot molecules is accumulated.

[a] *Georg-August-Universität Göttingen, Institut für Physikalische Chemie, Tammannstr. 6, 37077 Göttingen, Germany*

[b] *Universität Siegen, Physikalische Chemie 2, Adolf-Reichwein-Str. 2, 57076 Siegen, Germany. E-mail: lenzer@chemie.uni-siegen.de, oum@chemie.uni-siegen.de; Fax: +49 271 740 2943; Tel: +49 271 740 2803*

[c] *Max-Planck-Institut für biophysikalische Chemie, Am Faßberg 11, 37077 Göttingen, Germany*

† Electronic supplementary information (ESI) available: Synthesis of β-apo-4′-carotenal and torularhodinaldehyde; Fig. S1 featuring a comparison of S* signals for β-carotene, torularhodinaldehyde and β-apo-4′-carotenal. See DOI: 10.1039/c4cp05600k

1. Introduction

Photoexcitation of a carotene in the blue-green spectral region provides access to its optically bright second electronically excited state $S_2(1^1B_u^+)$. The subsequent dynamics of carotenoids in solution and in light-harvesting arrangements have been interpreted in the framework of various kinetic models involving different electronic states, with several of them still being the subject of considerable debate.[1,2] The simplest model for the intramolecular nonradiative relaxation of a carotenoid considers only two consecutive internal conversion (IC) steps *via* the $S_1(2^1A_g^-)$ to the $S_0(1^1A_g^-)$ state, as shown in Fig. 1(A). In this simplest case, modeling the optical response of such a kinetic system would require only three species-associated spectra (SAS) for S_0, S_1 and S_2 and the time constants τ_2 and τ_1 for the two IC processes.

However, the situation is indeed much more complicated: firstly, the SAS of all species S_i ($i = 0–2$) depend on the excess energy in the respective state: ''Vibrationally hot'' molecules S_i* show characteristic and complex spectral changes, including an increase of absorption at the red edge of the electronic band and a decrease of absorption maxima. This has been shown in a number of previous studies on molecules in the gas phase and

10478 | *Phys. Chem. Chem. Phys.,* 2015, **17**, 10478–10488

This journal is © the Owner Societies 2015

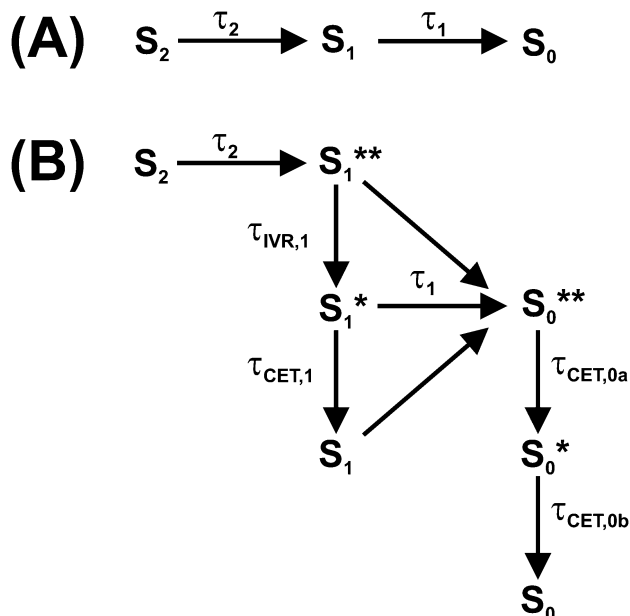Fig. 1 Two kinetic schemes for the interpretation of carotenoid photophysics. Horizontal and tilted arrows denote electronic transitions between different singlet states, whereas vertical arrows denote intramolecular vibrational redistribution or vibrational cooling by collisional energy transfer to the surrounding solvent.

in solution, such as azulene, anthracene and carotene derivatives.[3–7] Due to collisional energy transfer (CET) to the surrounding solvent molecules, the SAS will change with a characteristic time constant τ_{CET}, typically in the range 7–15 ps for standard organic solvents.[4,6,7] In addition, it has to be kept in mind that a simple single exponential decay of a transient absorption signal due to CET can only be expected if the absorption coefficient of the relaxing molecule linearly depends on its internal energy and at the same time the average energy transferred per collision $\langle \Delta E \rangle$ linearly depends on internal energy.[4]

Secondly, even for a fixed energy in an electronic state, the way the energy is distributed among the different vibrational modes might severely affect the appearance of the SAS. For instance, IC of a carotene from S_2 to S_1 initially produces an excited S_1 state with a non-statistical energy distribution. The energy will "randomize" over time, eventually leading to a statistical distribution (provided the electronic state lives long enough). This process is well-known as "intramolecular vibrational redistribution (IVR)".[5,8] It is accompanied by considerable spectral changes of the SAS[9,10] because energy will be "reshuffled" between optically "dark" and "bright" modes.

Thirdly, the IC time constants τ_i ($i = 1, 2$) may also vary with internal energy in the respective state S_i. For instance, it is well known from molecular beam experiments that IC rate constants increase with excess energy, e.g. by two or more orders of magnitude in the case of azulene in the S_2 and toluene in the S_1 state, when their excess energy is raised from 0 to 10 000 cm^{-1}.[11,12]

A complete description of such a kinetic system is complicated, because the SAS of each species S_i smoothly changes with its internal energy (as probably also does its lifetime).

We recently introduced a simplified kinetic treatment where such spectral changes are modeled by using time-dependent SAS. This way, IVR in S_1 and collisional relaxation of the hot ground state S_0* of β-carotene derivatives was successfully described.[6,7]

Alternatively, following an Occam's razor approach, one may resort to a simplified kinetic scheme with a sufficient number of species (with static SAS) and time constants to describe the essentials of the dynamics, leading us to the scheme in Fig. 1(B): after photoexcitation to S_2, a "hot" S_1** species[9,10] is quickly formed by IC (typically $\tau_2 < 200$ fs).[1] S_1** experiences fast IVR forming an isoenergetic S_1* species with a different spectrum. For β-carotene derivatives in n-hexane, one expects a time constant $\tau_{IVR,1}$ in the range 400–600 fs.[7] Collisional relaxation $\tau_{CET,1}$ is expected to be much slower than IVR, as already mentioned, in the 7–15 ps range. Therefore, the sequential relaxation scheme within S_1 should be accurate enough.

The relaxation processes within S_1 compete with electronic relaxation to the ground electronic state by IC. As noted above, IC of the isoenergetic S_1** and S_1* species is possibly faster than for the relaxed S_1 species, because of their higher internal energy. Nevertheless, due to the fact that energy dependent τ_1 values are not yet experimentally available for carotenoids, we assume here the same IC time constant τ_1 for all three S_1 species. IC accesses a vibrationally "hot" S_0 species, denoted as S_0**. Especially for short lifetimes τ_1 of the S_1 state, description of the spectral development of the hot ground state by a single spectrum might not be sufficient, and therefore we also consider here a slightly cooled-down species S_0*. Note that the spectral shape of the hot ground state species in reality smoothly varies with excess energy.[4,5] Relaxation of a carotenoid by collisional energy transfer to the solvent is then described by two collisional cooling time constants $\tau_{CET,0a}$ and $\tau_{CET,0b}$, respectively. The scheme in Fig. 1(B) will serve as the basis for describing the carotenoid systems studied here.

It should be noted that additional spectral features have been observed which have been assigned to different intermediates formed during the electronic relaxation of carotenoids. For instance, the S* signal was observed which is still under debate.[2,6,7,13] Others and we identify this S* signal as the vibrationally hot ground electronic state (S_0**/S_0*) discussed above,[6,7,14–18] Alternatively, S* has been either described as an electronically excited state,[18–24] different S_0 conformers,[25,26] or the vibrationally hot S_1 state.[27]

In our previous investigations of β-carotene and 13,13′-diphenyl-β-carotene, we presented strong evidence that the S* spectral features found in broadband transient absorption experiments arise from the characteristic absorption of vibrationally "hot" carotene molecules in S_0 which are generated by IC from the S_1 state, i.e. the S_0**/S_0* species in Fig. 1(B).[6,7] These species showed the typical "hot band" absorption on the red edge of the $S_0 \rightarrow S_2$ absorption band and a characteristic "finger-type" structure in the $S_0 \rightarrow S_2$ ground-state bleach (GSB). Both result from the subtraction of the "cold" (298 K) GSB spectrum from the transient "hot" spectra of the S_0**/S_0* molecules. This interpretation was strongly supported by the result of steady-state temperature-dependent absorption spectra, which nicely reproduced the difference spectra in the transient absorption
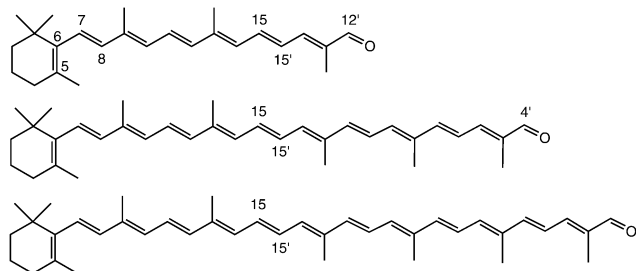
Fig. 2   Chemical structure of β-apo-12′-carotenal ($C_{25}H_{34}O$, top), β-apo-4′-carotenal ($C_{35}H_{46}O$, middle) and torularhodinaldehyde ($C_{40}H_{52}O$, bottom).

experiments, including the "hot band" absorption and the "finger-type" structure.[6]

Here, we provide additional strong support for this mechanism and the relaxation scheme in Fig. 1(B) by a systematic study of S_0**/S_0* spectral features for three all-*trans* apocarotenals featuring increasing conjugation lengths (Fig. 2). This way, the S_1 lifetime and thus the time constant τ_1 for generating S_0**/S_0* population *via* IC from S_1 can be precisely varied in wide ranges.[1,28] On the other hand, it is a well-known fact that time constants of collisional relaxation τ_{CET} in solution do not strongly depend on the type of the vibrationally excited molecule (*e.g.* 10–13 ps in the case of azulene in *n*-alkanes).[4,6,7] Therefore one should be able to "tune" the intensity and spectral shape of the S_0* state spectral features by variation of the conjugation length of the apocarotenal. As will be shown below, we indeed observe exactly such a behavior in the apocarotenal systems and therefore believe that the spectral features of S* arise from vibrationally hot molecules in the ground electronic state.

2. Experimental

2.1   Chemicals

The structure of the three all-*trans* apocarotenals β-apo-12′-carotenal (C25 aldehyde), β-apo-4′-carotenal (C35 aldehyde) and 3′,4′-didehydro-β,ψ-caroten-16′-al (C40 aldehyde, "torula-rhodinaldehyde") are shown in Fig. 2. β-Apo-12′-carotenal was a generous gift from BASF SE (Dr Hansgeorg Ernst) and used as received (purity > 97%). The other two apocarotenals were synthesized by repeated extension of the polyene chain *via* Wittig reaction of β-apo-8′-carotenal (C30 aldehyde) and a C5 phosphonium salt (both also generous gifts by Dr Hansgeorg Ernst from BASF SE). Details of the synthesis and purification procedures can be found in the ESI.† All experiments were performed in the solvent *n*-hexane (Merck Uvasol).

2.2   Pump–supercontinuum probe (PSCP) spectroscopy

Ultrafast broadband transient absorption experiments were carried out using our setup for pump–supercontinuum probe (PSCP) spectroscopy.[7,29–32] The apocarotenal sample was excited by a NOPA (λ_{pump} = 490 or 500 nm, beam diameter *ca.* 250 μm, energy *ca.* 1.0–1.5 μJ pulse^{-1}) and probed by a supercontinuum (350–770 nm, beam diameter *ca.* 150 μm), with the relative

polarization set at magic angle. The pump–probe intensity cross-correlation time was *ca.* 90 fs, with a time zero accuracy of *ca.* 10 fs. To avoid any influence of photoinduced sample degradation, 10–15 mL of an apocarotenal solution in *n*-hexane was circulated through a flow cell (path length 400 μm, window thickness 200 μm), so that the sample volume was exchanged after each pump–probe experiment (repetition frequency 920 Hz). Solutions with an OD (at maximum, 400 μm path length) of 0.333 (β-apo-12′-carotenal), 0.174 (β-apo-4′-carotenal) and 0.752 (torularhodinaldehyde) were employed. For these conditions, the transient absorption signals were in the linear regime, as confirmed in separate experiments. Steady-state absorption spectra of the sample solutions were recorded on a Varian Cary 5000 dual-beam spectrometer.

2.3   Global analysis procedure

The PSCP spectra were chirp-corrected by using the transient response of the pure *n*-hexane solvent. The spectra were then subjected to kinetic modeling. Each data set, which consisted of 512 kinetic traces, was analyzed globally using the kinetic schemes discussed below. Each species-associated spectrum was represented by a sufficiently large number of Gaussian functions, and only the known S_0 spectrum was kept fixed. During the fitting procedure, all parameters (position, width, height of the Gaussian functions and time constants of the kinetic model) were optimized simultaneously to arrive at the best fit, which also considered the experimentally determined time resolution by a convolution procedure.

3. Results and discussion

3.1   Steady-state absorption spectra

Fig. 3 shows steady-state absorption spectra of the three apocarotenals in *n*-hexane solution at 298.15 K. Upon extension of the polyene chain, there is a clear red-shift of the $S_0 \rightarrow S_2$ band
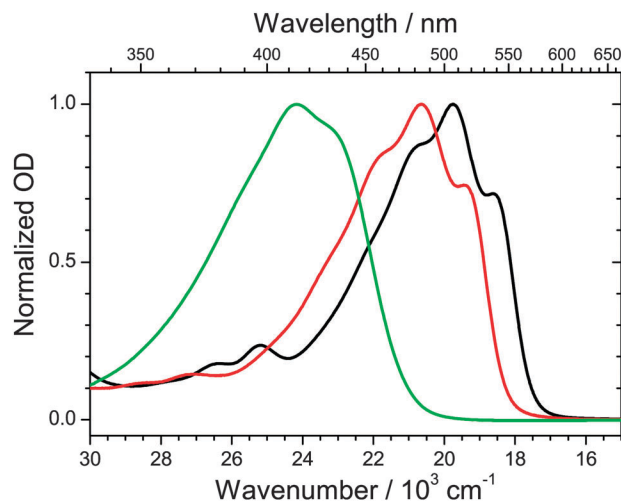

Fig. 3   Steady-state absorption spectra of β-apo-12′-carotenal (green), β-apo-4′-carotenal (red) and torularhodinaldehyde (black) in *n*-hexane at 298.15 K.

of the apocarotenals, suggesting a reduction of the S_0–S_2 energy gap. At the same time, the structure of the electronic band becomes more pronounced. The latter can be explained by a reduced influence of the terminal β-ionone ring on the absorption properties of the carotenes, as suggested by Christensen *et al.*:[33] according to their "distribution of conformers" model, conformations featuring different torsional angles C5–C6–C7–C8 (Fig. 2) of the β-ionone ring with respect to the rest of the polyene system, result in different "effective conjugation lengths", and thus a distribution of transition energies. The impact of this effect will be much weaker for a larger number of conjugated double bonds, thus the spectra will show more structure and appear more resolved.

3.2 Ultrafast dynamics of torularhodinaldehyde

We commence with the PSCP transient absorption data for torularhodinaldehyde in *n*-hexane, shown in Fig. 4. The carotene was excited at 500 nm ($S_0 \rightarrow S_2$ band). The top panel shows the dynamics around $t = 0$. We observe a pronounced bleach of the

Fig. 4 Transient PSCP absorption spectra of torularhodinaldehyde in *n*-hexane for excitation at 500 nm: (upper panel) −0.2–0 ps with 20 fs steps; (middle panel) 0.05–0.45 ps with 50 fs steps; (lower panel) 0.5–3 ps and 4–10 ps with 0.5 ps and 2 ps steps, respectively, and 18 ps. Selected transient spectra are shown as thick colored lines for guidance. For comparison, the inverted and scaled steady-state absorption spectrum is shown in the lower panel as an orange dotted line. The inset in the bottom panel shows a magnification of the spectra at 10 and 18 ps.

ground electronic state centered at 510 nm. In addition, absorption features appear in the 570–770 nm range. We assign these to $S_2 \rightarrow S_n$ excited state absorption (ESA), in agreement with our earlier PSCP experiments on other carotene systems.[6,7,31] The wavelength range below 450 nm appears to be spectrally silent, however, based on the inverted steady-state absorption spectrum, shown in the bottom panel as a dotted orange line, it is clear that there must be superimposed broad and unstructured $S_2 \rightarrow S_n$ ESA in this wavelength range compensating the bleach.

In the middle panel, the spectral development up to 0.45 ps is depicted. One observes the rise of a strong $S_1 \rightarrow S_n$ ESA band above 560 nm, as a result of $S_2 \rightarrow S_1$ internal conversion (IC) with a time constant $\tau_2 = 200$ fs, obtained from a global analysis procedure. The value is reasonable, compared with our earlier values found for β-carotene derivatives (160 fs), yet it could be also shorter, as the spectral dynamics could be "contaminated" by fast relaxation processes of the nascent S_1^{**} state due to IVR. While there is a slight narrowing of the S_1 ESA band, a separate time constant $\tau_{IVR,1}$ cannot be reliably determined. The region below 450 nm remains spectrally silent. This suggests that there is an $S_1 \rightarrow S_n$ ESA band which must be similarly unstructured and weak as in the case of the S_2 state.

The bottom panel shows the dynamics on longer timescales. Starting from 0.5 ps (black line), the absorption band decays in a non-uniform way: the peak centered at 600 nm quickly disappears, and what remains is a relatively broad absorption in the range 550 to 650 nm, see *e.g.* the green spectrum at 4 ps. We assign this process to IC from S_1 with a time constant $\tau_1 = 1.2$ ps. In addition, the peaks in the bleach region are more and more sharpening. Based on our previous findings for β-carotene derivatives,[6,7] we assign the remaining spectral features to the almost pure difference spectrum of vibrationally hot S_0 molecules which are generated by the fast IC process. The shape of this spectrum is explained as follows: first, a spectral hallmark of such species is a "hot-band" absorption (resulting from absorption of the population in the "Boltzmann tail") which should appear on the red edge of the room-temperature electronic spectrum (compare Fig. 3). Indeed, a pronounced absorption "bump" is located between 570 and 650 nm, see also the inset in the bottom panel of Fig. 4 for the spectra at 10 ps (blue line) and 18 ps (red line). The structured bleach in the 470–570 nm region results from another typical spectral property of vibrationally hot molecules, namely a decrease of spectral maxima and increase of spectral minima compared to room temperature spectra, see *e.g.* previous temperature-dependent gas-phase studies of the electronic spectra of azulene and anthracene by Schwarzer and co-workers[5] and our previous temperature dependent study of β-carotene steady-state absorption spectra in solution.[6] Subtraction of the room-temperature steady-state absorption spectrum from a transient spectrum will therefore result in a pronounced undulatory structure in the bleach region. This is also clearly seen in the inset of the bottom panel in Fig. 4 for the spectra at 10 and 18 ps. The "modulation depth" of the maxima and minima in the two transient spectra is much stronger than for the room temperature spectrum (orange dotted line in the bottom panel).
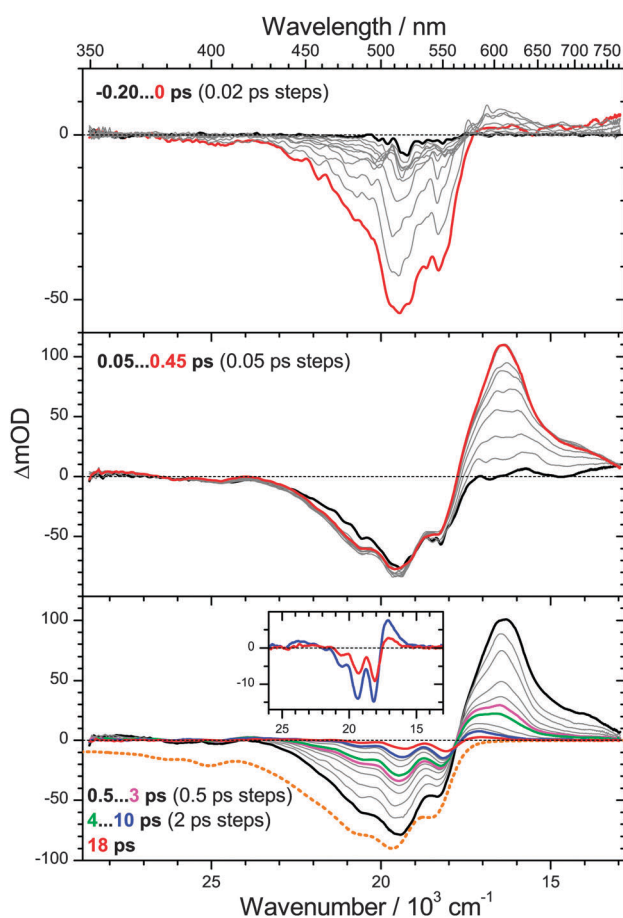
Its short S_1 lifetime makes torularhodinaldehyde a textbook example for studying S_0^* collisional energy transfer of carotenoids in solution. As shown in more detail below, collisional relaxation in the ground electronic state can be modeled best by employing two "hot" species S_0^{**} and S_0^* in the global kinetic analysis, relaxing with time constants of 3.4 and 10.5 ps, respectively. The second time constant agrees well with our previous findings for β-carotene derivatives in the same solvent: 11.9 ps for β-carotene[6] and 10.4 ps for 13,13′-diphenyl-β-carotene.[7] In the latter two cases, the S_0^* state features were weaker, because of the seven times larger S_1 lifetime ($\tau_1 = 8.7$ and 9.2 ps, respectively), and the correspondingly smaller S_0^* transient absorption features. The cooling time constant of S_0^* of torularhodinaldehyde also compares well with vibrational relaxation time constants of smaller organic molecules, such as azulene, where one finds $\tau_{CET,0} = 10$–13 ps for a series of alkanes.[4]

3.3 Photoinduced dynamics of β-apo-4′-carotenal

To further test the aforementioned generation and cooling mechanism of S_0^* molecules, we examined the photoinduced dynamics of β-apo-4′-carotenal in *n*-hexane. This carotenoid possesses the same type of chromophore as torularhodinaldehyde, yet the conjugated polyene system is slightly shorter. This should lead to a longer S_1 lifetime, as already suggested by results from our previous single-wavelength pump–probe studies in various solvents.[28]

PSCP spectra are shown in Fig. 5. In the top panel, the early-time dynamics around $t = 0$ are similar to those for torularhodinaldehyde, with pronounced $S_0 \rightarrow S_2$ bleach features centered at 500 nm and weak $S_2 \rightarrow S_n$ ESA above 600 nm. In the middle panel, the formation of $S_1 \rightarrow S_n$ ESA is observed, with a time constant $\tau_2 = 180$ fs, again very similar to torularhodinaldehyde. However, we note that the peak of the bleach and the S_1 ESA are shifted to the blue by *ca.* 840 cm^{-1} and 570 cm^{-1}, respectively, a result of the shorter conjugation length of β-apo-4′-carotenal.

The bottom panel depicts the behavior on longer time scales. The decay time of the S_1 ESA band (peak at 590 nm) is $\tau_1 = 4.9$ ps. The time constant of the $S_1 \rightarrow S_0^*$ IC process is thus by a factor of four larger than for torularhodinaldehyde. This becomes particularly clear in the inset, where the blue spectrum at 10 ps still shows a remainder of the S_1 ESA peak at 590 nm (in contrast to Fig. 4) overlapped by the characteristic signature of the vibrationally hot S_0^* molecules formed by the IC process. The "S_0^* part" of the transient spectrum at 10 ps shows the same fingerprints as in Fig. 4: a "hot band" absorption at 560 nm and a bleach which is much more structured than the ground state bleach of cold S_0 molecules. Importantly, the blue-shift of the S_0^* state difference spectra (840 cm^{-1}) is identical to the blue-shift of the $S_0 \rightarrow S_2$ steady-state absorption spectra, in agreement with the assignment to a hot ground-state species. The decay time of the S_0^* state feature obtained from global spectral analysis is $\tau_{CET,0} = 12.1$ ps, in line with the S_0^* collisional cooling time of torularhodinaldehyde.
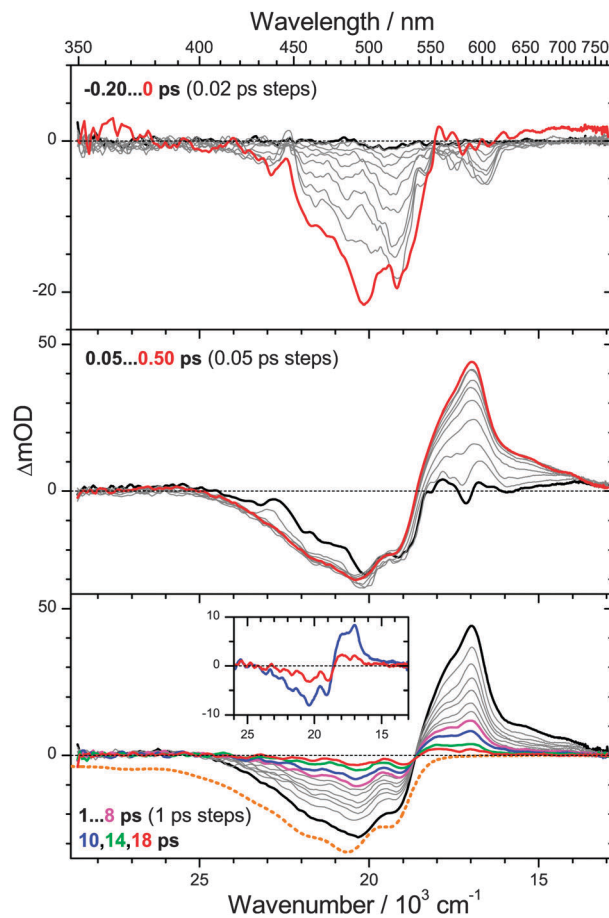

Fig. 5 Transient PSCP absorption spectra of β-apo-4′-carotenal in *n*-hexane for excitation at 500 nm: (upper panel) −0.2−0 ps with 20 fs steps; (middle panel) 0.05−0.50 ps with 50 fs steps; (lower panel) 1−8 ps with 1 ps steps and 10, 14 and 18 ps. Selected transient spectra are shown as thick colored lines for guidance. For comparison, the inverted and scaled steady-state absorption spectrum is shown in the lower panel as an orange dotted line. The inset in the bottom panel shows a magnification of the spectra at 10 and 18 ps.

3.4 Ultrafast dynamics of β-apo-12′-carotenal

So far, we have presented transient spectra for two apocarotenals where $\tau_1 < \tau_{CET,0}$, *i.e.* the S_0^* species are formed faster than they are cooled by collisions. As a result, pronounced transient spectral features of S_0^* were clearly identified. We now turn to an example, where $\tau_1 \gg \tau_{CET,0}$. In such a case, cooling of S_0^* molecules by collisions with solvent molecules is much faster than their generation from S_1. Thus, a detectable concentration of vibrationally hot S_0^* species in the ground electronic state is never accumulated and spectral features of S_0^* should be absent.

Experimentally, such conditions are established by further shortening the polyene chain of an apocarotenal, which largely increases τ_1,[28,34,35] whereas the time constant for collisional energy transfer τ_{CET} is much less sensitive to such a structural modification, as demonstrated by the results for torularhodinaldehyde and β-apo-4′-carotenal in this paper and previous experiments on a range of organic molecules.[4,36] Here, we therefore choose β-apo-12′-carotenal which features a rather short

10482 | *Phys. Chem. Chem. Phys.*, 2015, **17**, 10478–10488

This journal is © the Owner Societies 2015

conjugation length. In our previous preliminary studies on this molecule we found a lifetime τ_1 of *ca.* 200 ps,[34,35] therefore one expects $\tau_1 \approx 20 \cdot \tau_{CET,0}$ in this case.

PSCP spectra of β-apo-12′-carotenal in *n*-hexane (λ_{pump} = 490 nm) are presented in Fig. 6. The behavior at early times in the top panel is shown for the same delay times as in Fig. 4 and 5. Because of the much shorter conjugation length, the pronounced $S_0 \rightarrow S_2$ ground state bleach appears in the range 360–470 nm, in agreement with the steady-state absorption spectrum (Fig. 3). We note that the center peak at 430 nm is due to anti-Stokes Raman scattering of the C–H stretching modes of *n*-hexane and only present during temporal overlap of the pump and probe pulses. Above 470 nm, one observes $S_2 \rightarrow S_n$ ESA features, again blue-shifted compared to torularhodinaldehyde and β-apo-4′-carotenal.

In the middle panel one finds that the $S_2 \rightarrow S_n$ ESA quickly disappears due to ultrafast IC (τ_2 = 105 fs) and is replaced by a pronounced $S_1 \rightarrow S_n$ ESA band. The S_1 state undergoes further internal relaxation, as indicated by the green, blue and red lines
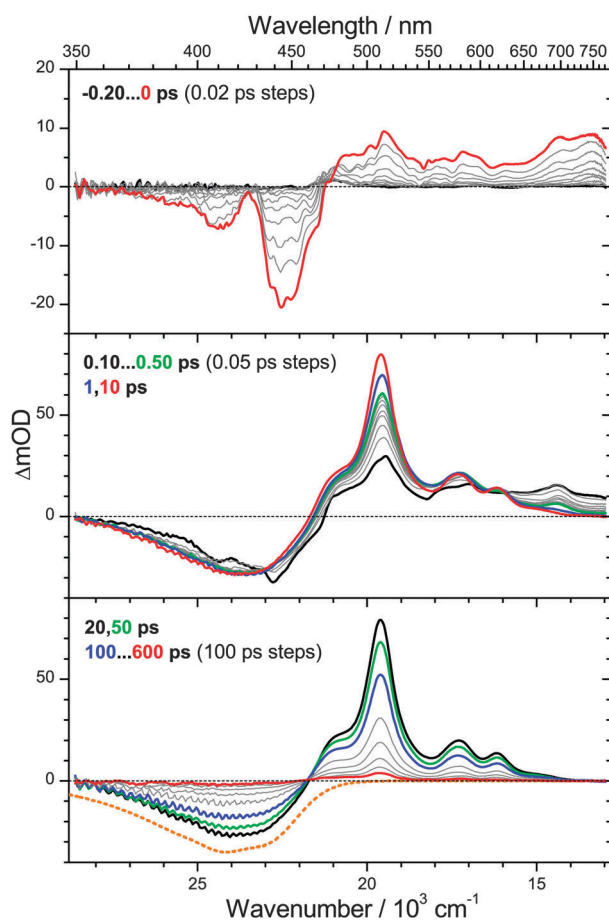
for delay times of 0.50, 1 and 10 ps, respectively. The ESA band becomes sharper, and especially the peak at 510 nm rises. We assign these dynamics to two processes: fast IVR of the initially prepared S_1** species with a time constant $\tau_{IVR,1}$ = 0.44 ps to form S_1*. The value is in very good agreement with values previously obtained by us for IVR timescales of β-carotene derivatives.[6,7] The second, slower, process is collisional deactivation of S_1* by the *n*-hexane solvent with a time constant of $\tau_{CET,1}$ = 8.3 ps. Note that the latter process is analogous to the $S_0^* \rightarrow S_0$ relaxation discussed above, however the initial vibrational excess energy of the S_1* molecules is of course lower and therefore the "hot band" dynamics in the S_1 state is less pronounced. Still it is clearly detectable for β-apo-12′-carotenal because its S_1 lifetime is much larger than for torularhodinaldehyde and β-apo-4′-carotenal.

In the bottom panel, one follows the slow $S_1 \rightarrow S_0$ IC process from the internally almost relaxed S_1 state with a time constant of 192 ps. The $S_1 \rightarrow S_n$ ESA band decays and at the same time the ground state bleach is filled up. There is an isosbestic point at 460 nm and, in contrast to the other two apocarotenals, we do not find indications for spectral features of S_0*.

3.5 Simplified kinetic schemes for apocarotenals in *n*-hexane

The transient PSCP spectra of the three apocarotenal systems were analyzed using simplified forms of the general scheme in Fig. 1(B). In the case of torularhodinaldehyde and β-apo-4′-carotenal we could not observe clear spectral indications of IVR of S_1**, except for a very minor narrowing of the S_1 band, which did not allow us to extract a reliable value for $\tau_{IVR,1}$. Also, because of the short IC lifetime τ_1, spectral indications for the collisional relaxation of S_1* are of course not present, and therefore a single S_1 species is sufficient for modeling the dynamics.

We simulate the results for torularhodinaldehyde employing the simplified sequential scheme in Fig. 7(A). Because of the very short S_1 lifetime of 1.2 ps, a substantial population of hot ground state molecules with initially high excess energy is quickly generated. Two vibrationally hot species S_0** and S_0* are

Fig. 6 Transient PSCP absorption spectra of β-apo-12′-carotenal in *n*-hexane for excitation at 490 nm: (upper panel) −0.2–0 ps with 20 fs steps; (middle panel) 0.10–0.50 ps with 50 fs steps, 1 ps and 10 ps; (lower panel) 20 ps and 50 ps, 100–600 ps with 100 ps steps. Selected transient spectra are shown as thick colored lines for guidance. For comparison, the inverted and scaled steady-state absorption spectrum is shown in the lower panel as an orange dotted line.
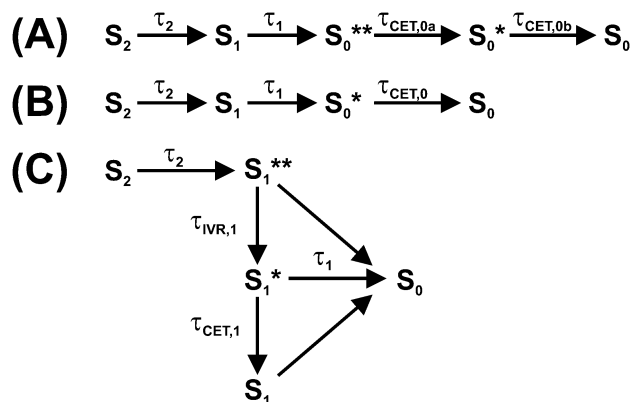

Fig. 7 Simplified kinetic schemes based on the general mechanism in Fig. 1(B) for interpreting the photophysics of the three apocarotenals in *n*-hexane. Relaxation schemes for (A) torularhodinaldehyde, (B) β-apo-4′-carotenal and (C) β-apo-12′-carotenal.
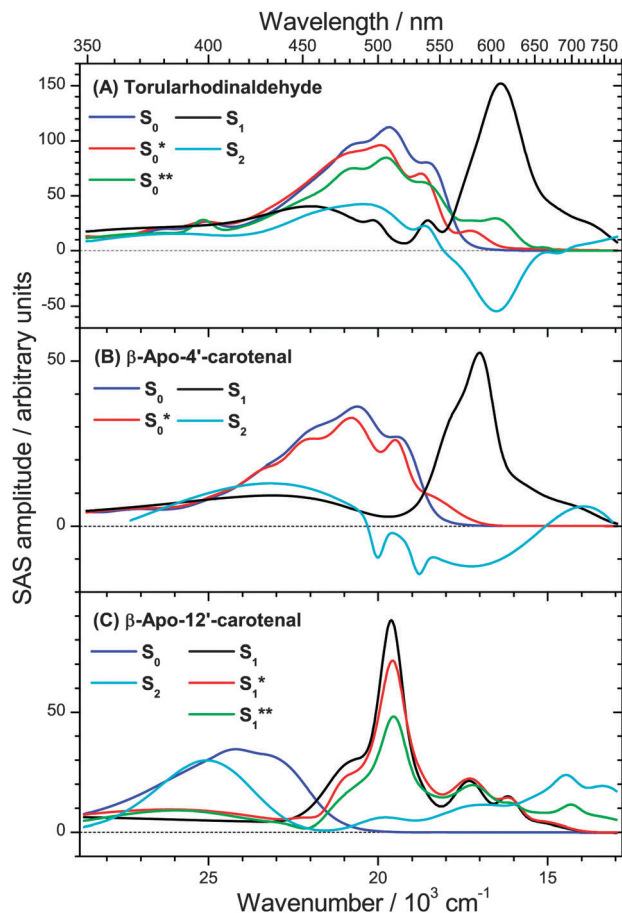
Fig. 8 Species-associated spectra (SAS) in *n*-hexane of (A) torularhodin-aldehyde, (B) β-apo-4′-carotenal and (C) β-apo-12′-carotenal.

Fig. 9 Kinetic traces for torularhodinaldehyde in *n*-hexane at (A) λ_{probe} = 501 nm, (B) λ_{probe} = 557 nm and (C) λ_{probe} = 585 nm.

employed to describe the complex change of the hot ground state spectrum resulting from vibrational cooling by solvent collisions. The corresponding SAS are shown in Fig. 8(A). Characteristic spectral changes due to collisional energy transfer are evident in the S_0^{**}, S_0^* and S_0 spectra (green, red and blue): the pronounced hot band at *ca.* 620 nm in the S_0^{**} spectrum disappears upon cooling and the spectrum narrows, leading to S_0^* which then further cools down to 298 K (S_0). Time constants of 3.4 and 10.5 ps are found for this collisional cooling process. Such biexponential dynamics is not unusual and expected if the absorption coefficient of S_0 does not linearly depend on excess energy.[4] The oscillator strength of the S_0 species is approximately conserved, as expected for a CET process. Note also that the spectral development is comparable to β-carotene derivatives, as previously reported by us in ref. 6 and 7. A similar spectral behavior of vibrationally hot ground state molecules is also observed for other organic molecules, compare *e.g.* the temperature-dependent absorption spectra for azulene and anthracene reported in Fig. 3 and 4 of ref. 5. This experimental evidence therefore supports our assignment of the S* spectral features[2] to vibrationally hot ground state molecules. Kinetic traces for three selected wavelengths are included in Fig. 9. They show the superposition of the fast S_1 decay dynamics with the collisional relaxation of the hot S_0^{**}/S_0^* species resulting in the curved
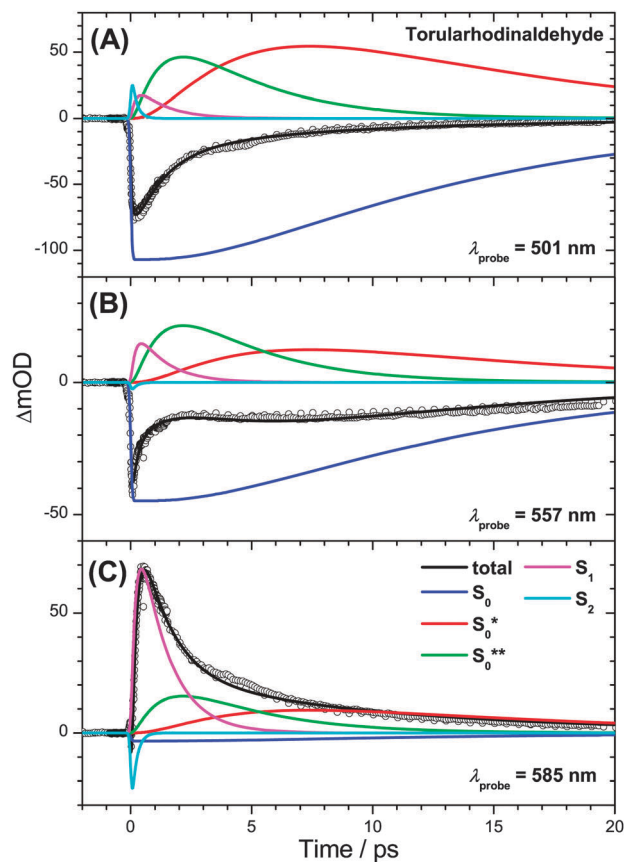
shape and the slow final decay of the transients. Global fit parameters are summarized in Table 1.

Our interpretation is further confirmed for β-apo-4′-carotenal. SAS can be found in Fig. 8(B). Because of the longer S_1 lifetime of τ_1 = 4.9 ps and the therefore slower production of hot ground state molecules, collisional cooling (τ_{CET} = 12.1 ps) competes more efficiently. As a result, the PSCP spectra can be fully modeled by considering the simplified kinetic scheme given in Fig. 7(B), including only a single (cooler) hot ground state species S_0^*. Note that the resulting SAS for S_0^* is very similar to the slightly cooled S_0^* species of torularhodinaldehyde. Three selected kinetic traces are shown in Fig. 10. Here, the longer lifetime of S_1 is evident (4.9 *vs.* 1.2 ps for torularhodinaldehyde), and therefore the S_1 decay is not as clearly separated from the cooling process of S_0^* as in the case of torularhodinaldehyde. A summary of global fit parameters is included in Table 1.

In the case of β-apo-12′-carotenal, IC from the S_1 state is very slow: $\tau_1 \gg \tau_{IVR,1}$, $\tau_{CET,1}$. As a result, IVR and CET in S_1 should be clearly observable. At the same time, this also means that $\tau_1 \gg \tau_{CET,0}$. Therefore, the steady-state approximation for S_0^* holds, and thus the concentration of S_0^* will be very small at all times. One therefore does not expect to see any S_0^* spectral features and thus the simplified scheme in Fig. 7(C) is applied. The resulting SAS are depicted in Fig. 8(C). Characteristic spectral changes accompany the relaxation within the S_1 state: the initially formed

Table 1 Kinetic parameters from global analysis for apocarotenals featuring different conjugation lengths in the solvent n-hexane

Carotenal	λ_{pump} (nm)	$\tau_{CC}{}^a$ (fs)	$\tau_2{}^b$ (fs)	$\tau_{IVR,1}$ and $\tau_{CET,1}{}^c$ (ps)	$\tau_1{}^d$ (ps)	$\tau_{CET,0a}$ and $\tau_{CET,0b}{}^e$ (ps)
Torularhodinaldehyde	500	90	200	—	1.2	3.4, 10.5
β-Apo-4′-carotenal	500	90	180	—	4.9	12.1
β-Apo-12′-carotenal	490	90	105	0.44, 8.3	192	—

[a] Pump–probe intensity cross-correlation of the experiment. [b] Internal conversion (IC) time constant for $S_2 \rightarrow S_1$, initially populating a hot S_1 state ($S_1{}^{**}$), which is not internally equilibrated. [c] Time constant for narrowing of the $S_1 \rightarrow S_n$ ESA band due to IVR (intramolecular vibrational redistribution; fast process) and CET (collisional energy transfer; slow process), not clearly assignable for torularhodinaldehyde and β-apo-4′-carotenal because of the short S_1 lifetime. [d] Internal conversion (IC) time constant populating the vibrationally hot ground electronic state. [e] Time constants for collisional energy transfer in the ground electronic state. Two time constants are required for torularhodinaldehyde, whereas for β-apo-4′-carotenal one time constant suffices. In the case of β-apo-12′-carotenal, IC from S_1 is very slow: thus the concentration of $S_0{}^*$ is very low and its contribution to the PSCP spectra too low to be detected.
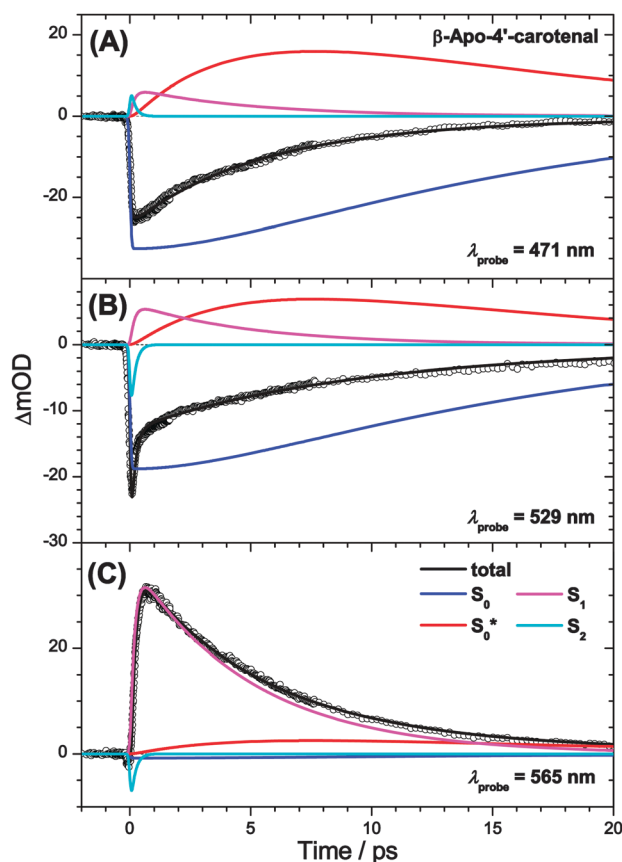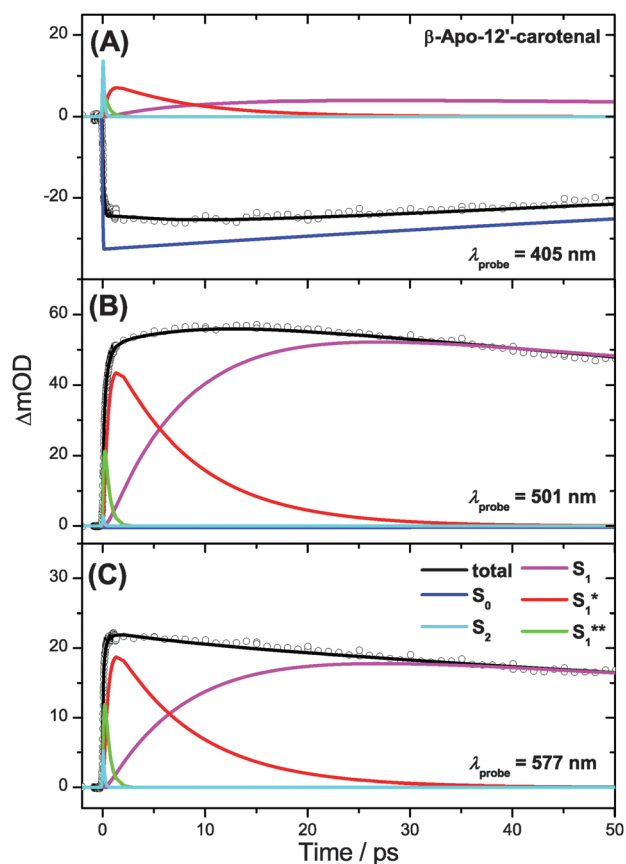

Fig. 10 Kinetic traces for β-apo-4′carotenal in n-hexane at (A) λ_{probe} = 471 nm, (B) λ_{probe} = 529 nm and (C) λ_{probe} = 565 nm.

$S_1{}^{**}$ species shows a broad spectrum (green line) extending to the upper wavelength limit of our spectral observation window, including a small but distinct peak at 700 nm. The main peak at 510 nm is already visible but it is small and broad, as is the rest of the spectrum. Due to fast IVR, an $S_1{}^*$ species is quickly formed ($\tau_{IVR,1}$ = 440 fs), which is internally equilibrated. This species exhibits a narrower spectrum and a steeper main peak (red line). $S_1{}^*$ then relaxes further by CET to the solvent to form the room temperature S_1 species (black line), with the aforementioned time constant τ_{CET} = 8.3 ps. Because of very slow IC to S_0 (τ_1 = 192 ps) we do not find spectral indications for an $S_0{}^*$ species which due to its extremely low concentration is below the detection limit.

Three representative kinetic traces are depicted in Fig. 11. CET in S_1 is apparent in the 501 nm transient as a characteristic round shape in the 2–30 ps range. Here the steepening of the main peak of the S_1 ESA band due to CET is superimposed by slow population loss due to IC to S_0. Kinetic parameters obtained from the global analysis are again summarized in Table 1.

The impact of vibrationally highly excited S_0 and S_1 species for the different apocarotenals is finally highlighted in Fig. 12, where PSCP spectra (open circles) and global analysis results (lines) are shown for the fixed delay time of 10 ps.

For torularhodinaldehyde (Fig. 12(A)), the S_1 population has already completely decayed (flat magenta line), and the structured

Fig. 11 Kinetic traces for β-apo-12′carotenal in n-hexane at (A) λ_{probe} = 405 nm, (B) λ_{probe} = 501 nm and (C) λ_{probe} = 577 nm.
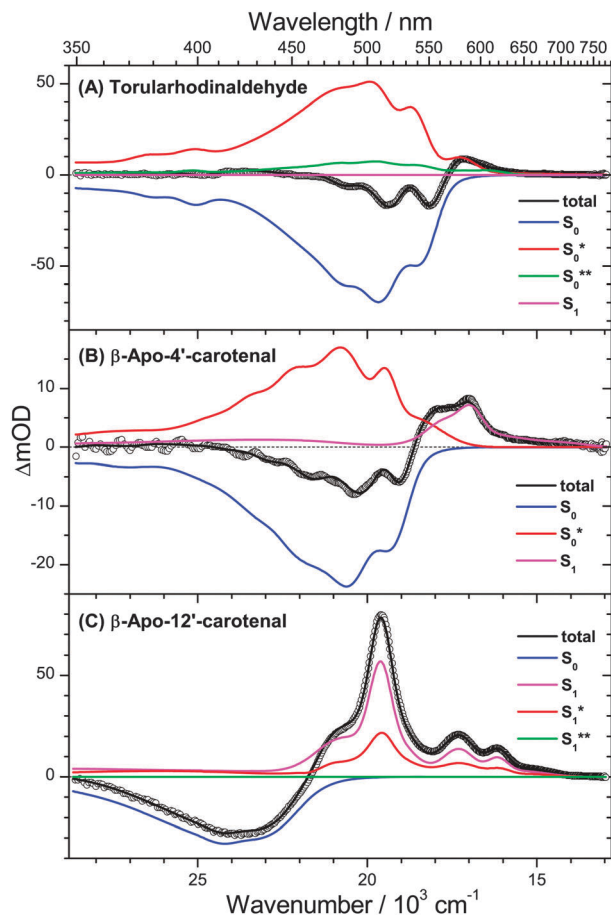
Fig. 12 PSCP spectra (circles) at 10 ps in *n*-hexane for (A) torularhodin-aldehyde, (B) β-apo-4′carotenal and (C) β-apo-12′-carotenal, including total fit and contributions from individual species.

spectrum is a result of the superposition of hot ground state absorption (mainly S_0^* (red), but also S_0^{**}(green)) and the bleach of room-temperature S_0 molecules (blue).

For β-apo-4′-carotenal (Fig. 12(B)), the resulting spectrum is a superposition of remaining S_1 absorption (magenta), hot ground state absorption of S_0^* (red) and the bleach of cold S_0 molecules (blue). The S_1 and S_0^* contributions are responsible for the characteristic broad double-peak structure in the range 560–590 nm, which we similarly observed previously for β-carotene and 13,13′-diphenyl-β-carotene,[6,7] which feature only a slightly longer S_1 lifetime (*ca.* 9 ps).

In the case of β-apo-12′-carotenal (Fig. 12(C)), the spectrum at 10 ps contains only ESA contributions from the S_1 and S_1^* species (CET in the first electronically excited state is still ongoing), which is superimposed by the bleach of cold S_0 molecules (blue). Because of the long S_1 lifetime (192 ps) the concentration of S_0^* molecules is negligible, and therefore spectral features of S_0^* are not visible at all.

4. Conclusions

We have demonstrated that three apocarotenals with very different S_1 lifetimes can be described by simplified versions

of the relaxation model in Fig. 1(B), considering only three electronic species S_2, S_1 and S_0 and additional "distortions" of their spectra due to internal vibrational excess energy or incomplete IVR (Fig. 7). These "spectral distortions" were captured in a simplified kinetic model by introducing vibrationally "hot" electronic species S_0^{**}, S_0^* and S_1^* and a not internally equilibrated S_1^{**} species. The visibility of these species in transient spectra depends on the specific value of the S_1 lifetime τ_1, *e.g.* if it is much larger or much smaller than typical time constants for collisional relaxation ($\tau_{CET} \approx 10$ ps). The spectral properties of the "hot" species found in our global analysis are completely consistent with experimental data in the literature for vibrationally hot organic molecules, *e.g.* showing a characteristic hot band absorption tail reaching by 1000–2000 cm^{-1} toward the red spectral range.[4,5] Moreover, in our previous study of β-carotene, the difference absorption spectrum of S_0^* was independently measured in separate temperature-dependent steady-state absorption experiments and found to be very similar to the S* spectral features in the transient absorption spectra.[6] The same characteristic spectral signatures are found in the current study for torularhodinaldehyde and β-apo-4′-carotenal, see Fig. 12(A) and (B), and this striking similarity is further highlighted in the comparison shown in Fig. S1 of the ESI.† We also believe that this model is applicable to a wide range of carotenoids. As one example, we already demonstrated in two previous studies that the photoinduced processes of two β-carotene derivatives are well described in the same way.[6,7] As another example, clear S_0^*-like spectral signatures were found by Gillbro and co-workers for the long-chain dodecapreno-β-carotene which features a very short S_1 lifetime of $\tau_1 = 0.5$ ps.[14] Its spectral features are very similar to those of torularhodinaldehyde.

Also, various observations from previous experimental transient absorption studies of carotenoids can be traced back to vibrationally hot ground state molecules: for instance, Papagiannakis *et al.*[37] and Savolainen *et al.*[38] found that the excitation intensity modified the intensity ratio between S* and S_1 absorption signals for carotenoids bound to natural and artificial light-harvesting complexes. In both cases, the S*/S_1 absorption ratio increased when the pump energy was increased and entered the nonlinear regime. Such a behavior can be traced back to the increasing influence of a two-photon excited population with high initial excess energy. After IC, such carotenoid molecules will enter S_0 with an excess energy much higher than for an initially one-photon excited population. The S_0^{**} spectrum of these molecules with high internal temperature will be considerably distorted giving rise to much stronger hot band absorption features than those of the one-photon excited S_0^* population.

In addition, Billsten *et al.* observed that the intensity of the S* signal of zeaxanthin was correlated with the amount of initial excess energy:[39] the S* absorption features became more pronounced when decreasing the excitation wavelength (485, 400 and 266 nm). This can be explained in the same way as above. For higher initial excitation energies, zeaxanthin will enter S_0 with much higher excess energy which gives rise to more pronounced S* absorption features.

10486 | *Phys. Chem. Chem. Phys.*, 2015, **17**, 10478–10488

This journal is © the Owner Societies 2015

We therefore believe that extensions of our kinetic model will be only required in special cases: for instance, systems such as β-apo-12′-carotenal are known to exhibit significant charge transfer character in polar solvents, including the appearance of substantial stimulated emission and a drastic reduction of the S_1 lifetime:[28,34,35,40,41] the first electronically excited state is then better termed "S_1/ICT",[42–44] but the basic model of three electronic states survives. Because formation of the S_1/ICT state leads to a substantial change in dipole moment, solvation dynamics will induce a transient Stokes shift of the S_1/ICT stimulated emission and possibly also excited state absorption features, as already demonstrated by us previously.[34] In the simplest approach, solvation dynamics can be handled *e.g.* by introducing an additional S_1 species in the models of Fig. 1(B) and 7 or by introducing a time-dependence for the S_1 spectrum, as demonstrated by us previously.[6,7] Short-chain apocarotenals, such as all-*trans*-retinal (= all-*trans*-β-apo-15-carotenal), might constitute another special class. In that case triplet formation (*via* an intermediate nπ* state) and *trans–cis* isomerization were proposed as additional channels.[41,45]

Acknowledgements

Notes and references

1 T. Polívka and V. Sundström, *Chem. Rev.*, 2004, **104**, 2021.

2 T. Polívka and V. Sundström, *Chem. Phys. Lett.*, 2009, **477**, 1.

3 L. Brouwer, H. Hippler, L. Lindemann and J. Troe, *J. Phys. Chem.*, 1985, **89**, 4608.

4 D. Schwarzer, J. Troe, M. Votsmeier and M. Zerezke, *J. Chem. Phys.*, 1996, **105**, 3121.

5 D. Schwarzer, C. Hanisch, P. Kutne and J. Troe, *J. Phys. Chem. A*, 2002, **106**, 8019.

6 T. Lenzer, F. Ehlers, M. Scholz, R. Oswald and K. Oum, *Phys. Chem. Chem. Phys.*, 2010, **12**, 8832.

7 K. Golibrzuch, F. Ehlers, M. Scholz, R. Oswald, T. Lenzer, K. Oum, H. Kim and S. Koo, *Phys. Chem. Chem. Phys.*, 2011, **13**, 6340.

8 D. J. Nesbitt and R. W. Field, *J. Phys. Chem.*, 1996, **100**, 12735.

9 H. H. Billsten, D. Zigmantas, V. Sundström and T. Polívka, *Chem. Phys. Lett.*, 2002, **355**, 465.

10 F. L. de Weerd, I. H. M. van Stokkum and R. van Grondelle, *Chem. Phys. Lett.*, 2002, **354**, 38.

11 U. Hold, T. Lenzer, K. Luther and A. C. Symonds, *J. Chem. Phys.*, 2003, **119**, 11192.

12 H. Frerichs, T. Lenzer, K. Luther and D. Schwarzer, *Phys. Chem. Chem. Phys.*, 2005, **7**, 620.

13 P. Chabéra, M. Fuciman, P. Hríbek and T. Polívka, *Phys. Chem. Chem. Phys.*, 2009, **11**, 8795.

14 P. O. Andersson and T. Gillbro, *J. Chem. Phys.*, 1995, **103**, 2509.

15 W. Wohlleben, T. Buckup, H. Hashimoto, R. J. Cogdell, J. L. Herek and M. Motzkus, *J. Phys. Chem. B*, 2004, **108**, 3320.

16 T. Buckup, J. Savolainen, W. Wohlleben, J. L. Herek, H. Hashimoto, R. R. B. Correia and M. Motzkus, *J. Chem. Phys.*, 2006, **125**, 194505.

17 V. Namboodiri, M. Namboodiri, G. Flachenecker and A. Materny, *J. Chem. Phys.*, 2010, **133**, 054503.

18 D. Kosumi, S. Maruta, T. Horibe, Y. Nagaoka, R. Fujii, M. Sugisaki, R. J. Cogdell and H. Hashimoto, *J. Chem. Phys.*, 2012, **137**, 064505.

19 C. C. Gradinaru, J. T. M. Kennis, E. Papagiannakis, I. H. M. van Stokkum, R. J. Cogdell, G. R. Fleming, R. A. Niederman and R. van Grondelle, *Proc. Natl. Acad. Sci. U. S. A.*, 2001, **98**, 2364.

20 D. M. Niedzwiedzki, J. O. Sullivan, T. Polívka, R. R. Birge and H. A. Frank, *J. Phys. Chem. B*, 2006, **110**, 22872.

21 D. Niedzwiedzki, J. F. Koscielecki, H. Cong, J. O. Sullivan, G. N. Gibson, R. R. Birge and H. A. Frank, *J. Phys. Chem. B*, 2007, **111**, 5984.

22 H. Cong, D. M. Niedzwiedzki, G. N. Gibson and H. A. Frank, *J. Phys. Chem. B*, 2008, **112**, 3558.

23 N. Christensson, F. Milota, A. Nemeth, J. Sperling, H. F. Kauffmann, T. Pullerits and J. Hauer, *J. Phys. Chem. B*, 2009, **113**, 16409.

24 A. E. Jailaubekov, S.-H. Song, M. Vengris, R. J. Cogdell and D. S. Larsen, *Chem. Phys. Lett.*, 2010, **487**, 101.

25 J. Hauer, M. Maiuri, D. Viola, V. Lukes, S. Henry, A. M. Carey, R. J. Cogdell, G. Cerullo and D. Polli, *J. Phys. Chem. A*, 2013, **117**, 6303.

26 V. Lukeš, N. Christensson, F. Milota, H. F. Kauffmann and J. Hauer, *Chem. Phys. Lett.*, 2011, **506**, 122.

27 E. E. Ostroumov, M. G. Müller, M. Reus and A. R. Holzwarth, *J. Phys. Chem. A*, 2011, **115**, 3698.

28 F. Ehlers, D. A. Wild, T. Lenzer and K. Oum, *J. Phys. Chem. A*, 2007, **111**, 2257.

29 K. Oum, P. W. Lohse, O. Flender, J. R. Klein, M. Scholz, T. Lenzer, J. Du and T. Oekermann, *Phys. Chem. Chem. Phys.*, 2012, **14**, 15429.

30 P. W. Lohse, J. Kuhnt, S. I. Druzhinin, M. Scholz, M. Ekimova, T. Oekermann, T. Lenzer and K. Oum, *Phys. Chem. Chem. Phys.*, 2011, **13**, 19632.

31 T. Lenzer, S. Schubert, F. Ehlers, P. W. Lohse, M. Scholz and K. Oum, *Arch. Biochem. Biophys.*, 2009, **483**, 213.

32 A. L. Dobryakov, S. A. Kovalenko, A. Weigel, J. L. Pérez Lustres, J. Lange, A. Müller and N. P. Ernsting, *Rev. Sci. Instrum.*, 2010, **81**, 113106.

33 R. L. Christensen, M. Goyette, L. Gallagher, J. Duncan, B. DeCoster, J. Lugtenburg, F. J. Jansen and I. van der Hoef, *J. Phys. Chem. A*, 1999, **103**, 2399.

This journal is © the Owner Societies 2015

Phys. Chem. Chem. Phys., 2015, **17**, 10478–10488 | **10487**

34 K. Oum, P. W. Lohse, F. Ehlers, M. Scholz, M. Kopczynski and T. Lenzer, *Angew. Chem., Int. Ed.*, 2010, **49**, 2230.

35 M. Kopczynski, F. Ehlers, T. Lenzer and K. Oum, *J. Phys. Chem. A*, 2007, **111**, 5370.

36 S. A. Kovalenko, R. Schanz, H. Hennig and N. P. Ernsting, *J. Chem. Phys.*, 2001, **115**, 3256.

37 E. Papagiannakis, I. H. M. van Stokkum, M. Vengris, R. J. Cogdell, R. van Grondelle and D. S. Larsen, *J. Phys. Chem. B*, 2006, **110**, 5727.

38 J. Savolainen, T. Buckup, J. Hauer, A. Jafarpour, C. Serrat, M. Motzkus and J. L. Herek, *Chem. Phys.*, 2009, **357**, 181.

39 H. H. Billsten, J. Pan, S. Sinha, T. Pascher, V. Sundström and T. Polívka, *J. Phys. Chem. A*, 2005, **109**, 6852.

40 F. Ehlers, T. Lenzer and K. Oum, *J. Phys. Chem. B*, 2008, **112**, 16690.

41 T. Polívka, S. Kaligotla, P. Chábera and H. A. Frank, *Phys. Chem. Chem. Phys.*, 2011, **13**, 10787.

42 J. A. Bautista, R. E. Connors, B. B. Raju, R. G. Hiller, F. P. Sharples, D. Gosztola, M. R. Wasielewski and H. A. Frank, *J. Phys. Chem. A*, 1999, **103**, 8751.

43 D. Zigmantas, T. Polívka, R. G. Hiller, A. Yartsev and V. Sundström, *J. Phys. Chem. A*, 2001, **105**, 10296.

44 D. Zigmantas, R. G. Hiller, A. Yartsev, V. Sundström and T. Polívka, *J. Phys. Chem. B*, 2003, **107**, 5339.

45 S. Yamaguchi and H. Hamaguchi, *J. Chem. Phys.*, 1998, **109**, 1397.

10488 | *Phys. Chem. Chem. Phys.*, 2015, **17**, 10478–10488

This journal is © the Owner Societies 2015